PROCEEDINGS OF SCIENCE

The Study of K$\to \mu\nu\gamma$ Decay at ISTRA+ Setup

Viacheslav Duk*
Institute for Nuclear Research of RAS, Moscow, Russia
E-mail: Viacheslav.Duk@cern.ch

The radiative decay $K^- \to \mu^- \nu_\mu \gamma$ has been studied at ISTRA+ setup in a new kinematical region $25MeV < E^\star_\gamma < 150MeV$. About 44000 events of $K^- \to \mu^- \nu_\mu \gamma$ have been observed. The sign and value of $F_V - F_A$ has been measured for the first time. The preliminary result is $F_V - F_A = 0.12 \pm 0.03(stat) \pm 0.04(syst)$.

2009 KAON International Conference KAON09,
June 09 - 12 2009
Tsukuba, Japan

*Speaker.

PoS(KAON09)036

1. Introduction

Radiative kaon decays are dominated by long distance (low energy) physics. For low energy processes there are no direct predictions from SM and effective theories such as Chiral pertubation theory (χPT) are used. χPT gives decay rates for most kaon decay modes. That is why radiative kaon decays provide a testing ground for χPT. Moreover, these decays are sensitive to New Physics.

The decay $K^- \to \mu^- \nu_\mu \gamma$ is sensitive to hadronic weak currents in low-energy region. The decay amplitude includes two terms: internal bremsstrahlung (IB) and structure dependent term (SD). IB contains radiative corrections from $K^- \to \mu^- \nu_\mu$. SD allows to probe electroweak structure of kaon.

The differential decay rate is calculated within ChPT and can be written in terms of standard kinematical variables x=$2E^\star_\gamma/M_k$ and $y = 2E^\star_\mu/M_k$ (see [1] for details). It includes IB, SD$\pm$ parts and their interference INT$\pm$. The contribution of SD$\pm$ and INT$\pm$ is determined by two formfactors F_V and F_A, namely SD$\pm$ (INT$\pm$) term in the decay differential rate is proportional to $|F_V \pm F_A|^2$ $(F_V \pm F_A)$. $(F_V \pm F_A)$ are calculated within χPT (O(p^4) [1], O(p^6) [2]) and LFQM model [3].

Experimentally, the decay $K^- \to \mu^- \nu_\mu \gamma$ was studied mostly in the IB dominated region (see [4],[5]). There was only one formfactor measurement in E787 experiment [4]. In this study, SD+ term was extracted and $|F_V + F_A|$ was obtained to be $|F_V + F_A| = 0.165 \pm 0.007(stat) \pm 0.011(syst)$. $F_V - F_A$ was measured by E865 in $K \to \mu\nu e^+ e^-$ decay [6]: $F_V - F_A = 0.077 \pm 0.028$. The goal of our study is to measure $F_V - F_A$ in $K \to \mu\nu\gamma$ decay in the kinematical region where INT- term (and hence $F_V - F_A$) can be extracted.

2. Experimental setup

The experiment has been performed at the IHEP 70 GeV proton synchrotron U-70. The experimental setup ISTRA+ (Fig.1) has been described in some details elsewhere[7].

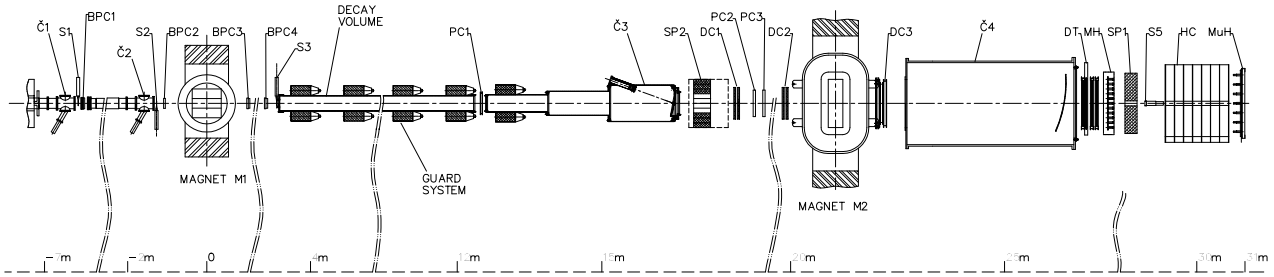

Figure 1: Elevation view of the ISTRA+ detector.

The setup is located in the negative unseparated secondary beam. The beam momentum in the measurements is ~ 26 GeV with $\Delta p/p \sim 1.5\%$. The admixture of K^- in the beam is $\sim 3\%$. The beam intensity is $\sim 3 \cdot 10^6$ per 1.9 sec U-70 spill. The beam particle deflected by M_1 is measured by $BPC_1 \div BPC_4$ (1mm step multiwire chambers), the kaon identification is done by $\check{C}_0 \div \check{C}_2$ threshold $\check{C}$-counters. The 9 meter long vacuumed decay volume is surrounded by 8 lead

glass rings $LG_1 \div LG_8$ used to veto low energy photons. SP_2 is a lead glass calorimeter to detect/veto large angle photons. The decay products deflected in M2 with 1Tm field integral are measured by $PC_1 \div PC_3$ (2mm step proportional chambers); $DC_1 \div DC_3$ (1cm cell drift chambers) and finally by 2cm diameter drift tubes $DT_1 \div DT_4$. Wide aperture threshold Cerenkov counters $\check{C}_3$, $\check{C}_4$ are filled with He and are not used in the present measurements. SP_1 (ECAL) is a 576-cell lead glass calorimeter, followed by HC - a scintillator-iron sampling hadron calorimeter. HC is subdivided into 7 longitudinal sections 7×7 cells each. MH is a 11×11 cell scintillating hodoscope used to improve the time resolution of the tracking system, MuH is a 7×7 cell muon hodoscope.

The trigger is provided by $S_1 \div S_5$ scintillation counters, $\check{C}_0 \div \check{C}_2$ Cerenkov counters, analog sum of amplitudes from the last dinodes of the SP_1 : $T = S_1 \cdot S_2 \cdot S_3 \cdot \bar{S}_4 \cdot \check{C}_0 \cdot \bar{\check{C}}_1 \cdot \bar{\check{C}}_2 \cdot \bar{S}_5 \cdot \Sigma(SP_1)$, here S_4 is a scintillator counter with a hole to suppress beam halo ; S_5 is a counter downstream the setup at the beam focus; $\Sigma(SP_1)$- a requirement for the analog sum of ECAL amplitudes to be above ∼700 MeV - a MIP signal. The last requirement serves to suppress the $K \to \mu\nu$ decay.

3. Event selection

The event selection criteria for K→ $\mu\nu\gamma$ are organized in several groups:
- K→ $\mu\nu\gamma$ signature;
- quality of beam and secondary tracks;
- photon energy and veto;
- vertex characteristics;
- additional general cuts.

3.1 K→ $\mu\nu\gamma$ signature

The decay is identified as follows: one primary track (kaon), one negatively charged secondary track, μ flag in HCAL; one shower in ECAL not associated with the charged track. Muon identification using HCAL is described in our previous papers and includes the following cuts:
$E_{ecal} > 200$;
$1 < E_{hcal} < 200$;
$E_{h3}/E_{hcal} > 0.05$
where E_{ecal} is the energy in ECAL around charged track, E_{hcal} - energy deposited in HCAL and E_{h3} is the energy released in the first 3 layers of HCAL.

3.2 Quality of beam and secondary tracks

Several cuts are applied to clean the data:
- no positively charged secondary particles;
- number of beam and decay tracks in both X and Y projections is equal to 1;
- CL of primary tracks in both X and Y projections must be greater than 10^{-2};
- CL of decay tracks is greater than 0.1 (decay-X) and 0.15 (decay-Y);
- the angle between primary (kaon) and secondary (muon) tracks is greater than 2 mrad.

3.3 Photon energy and veto

Cuts containing photon energy include:
- Gamma energy in kaon rest frame is greater than 10 MeV;
- no photons in SP2 calorimeter (energy threshold is 0.5 GeV for total energy release);
- no photons in GS.

3.4 Vertex characteristics

For vertex characteristics we have the following requirements:
- z-coordinate must be within the interval $400 < z < 1600$cm, where decay volume is located between 300 and 1200cm and 1650cm is the coordinate of the SP2 veto calorimeter;
- $(-3) < x_{vertex} < 3$cm;
- $(-2) < y_{vertex} < 6$cm;
- CL of general vertex fit is greater than 10^{-2}.

3.5 Additional general cuts

Additional cuts are applied to suppress backgrounds:
- number of hits in matrix hodoscope (MH) is less than 3;
- missing momentum does not point to the ECAL central hole (this cut effectively rejects Kπ2 background since missing particle is the lost photon in this case);
- the angle between primary (kaon) and secondary (muon) tracks is less than 20 mrad;
- the difference of y-coordinate between muon track extrapolation to ECAL and a shower centre is $(-20)\text{cm} < \Delta y_{\mu\gamma} < 50$cm.

4. Signal observation and background

Main background comes from 2 decay modes: $K^- \to \mu^- \nu \pi^0 (K\mu 3)$ and $K^- \to \pi^- \pi^0 (K\pi 2)$ with one gamma lost from $\pi^0 \to \gamma\gamma$ and π misidentified as μ. Distribution over $M(\mu\nu\gamma)$ is used for signal observation. $M^2(\mu\nu\gamma) = (P_\mu + P_\nu + P_\gamma)^2$ where P_μ, P_ν, P_γ are 4-momenta of corresponding particles; missing mass is supposed to be equal to 0 so that $\vec{p}_\nu = \vec{p}_K - \vec{p}_\mu - \vec{p}_\gamma; E_\nu = |\vec{p}_\nu|$. $M(\mu\nu\gamma)$ peaks at K^- mass for the signal.

5. Signal extraction

To extract signal, the following procedure is applied:
- all kinematical (x,y) region is divided into strips on x (x-strips), $\Delta x = 0.05$;
- we look at y and $M(\mu\nu\gamma)$ in each x-strip;
- we make a cut on y in each x-strip (xy-strip) to minimize background under signal peak in $M(\mu\nu\gamma)$ distribution;
- xy-strips with significant signal peak are selected for further analysis;
- Fitting $M(\mu\nu\gamma)$ in xy-strips gives the number of $K^- \to \mu^- \nu\gamma$ events (the shape of background and signal distribution is taken from MC). In fig. 2 one can see the distribution over $M(\mu\nu\gamma)$ in one of xy-strips. The signal peak is clearly seen.

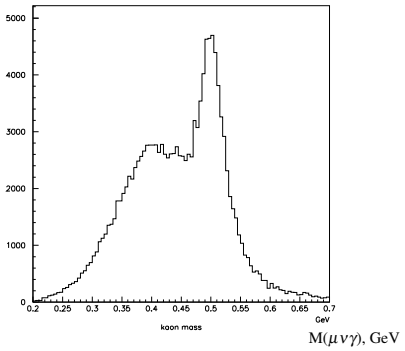

Figure 2: *M(μνγ) for xy-strip, real data*

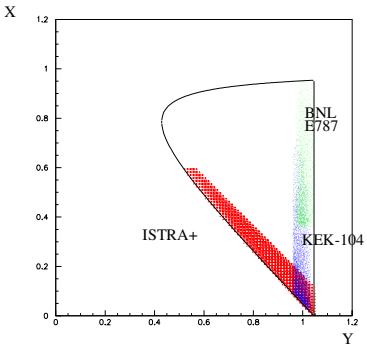

Figure 3: *$x=2E^{\star}_{\gamma}/M_k$, $y=2E^{\star}_{\mu}/M_k$ ISTRA+(red); BNL E787(green);KEK-104(blue)*

For the further analysis we selected xy-strips with width $\Delta y \sim 0.1$ near kinematical border (see fig. 3) in the following region: $0.1 < x < 0.6$ which corresponds to $25MeV < E^{\star}_{\gamma} < 150MeV$. The total number of $K^- \to \mu^- \nu\gamma$ events is ∼44000. Our kinematical region is complementary to that of previous experiments[4],[5] (fig. 3).

6. $F_V - F_A$ measurement

6.1 General idea

The distribution over $M(\mu^- \nu_\mu \gamma)$ is the same for IB and INT- terms in xy-strips. That is why we can compare event number obtained from data with IB prediction. The deviation will give INT- value and sign.

6.2 Extraction procedure

For each xy-strip we have experimental event number N_{exp} from data and IB event number N_{IB} from MC. Then we plot N_{exp}/N_{IB} as a function of x where each bin corresponds to a certain xy-strip (see fig. 4).

For IB only we would have constant. It is the case for small x where IB is dominated and INT- is negligible. For large x we see that N_{exp} also includes negative interference term. We fit N_{exp}/N_{IB} distribution with $p_1 * [(f_{IB}(x) + f_{INT-}(x, p_2))/f_{IB}(x)]$ where fit parameters p_1 and p_2 correspond to normalization constant and $F_V - F_A$ respectively (in the present analysis F_V and F_A are assumed to be constant). The result of the fit is as follows: $F_V - F_A = 0.12 \pm 0.03(stat)$.

7. Systematic error estimation

The main sources of systematic error come from the choice of cut value on x and y and from the spectrum shape of signal and background. With the current estimation of systematic error we finally get our preliminary result:
$F_V - F_A = 0.12 \pm 0.03(stat) \pm 0.04(syst)$.
The detailed analysis of systematics is in progress.

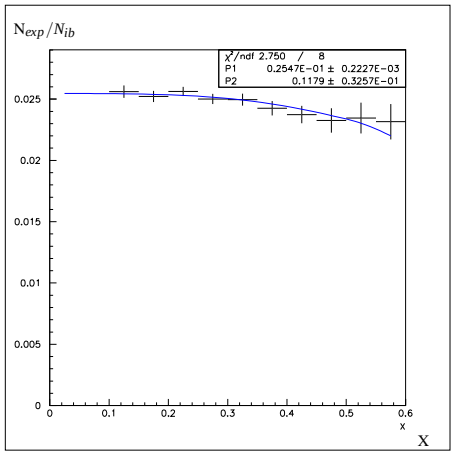

Figure 4: N_{exp}/N_{ib} *for xy-strips*

8. Conclusion

The radiative decay $K^- \to \mu^- \nu_\mu \gamma$ has been studied using in-flight decays at ISTRA+ setup. About 44000 events of $K^- \to \mu^- \nu_\mu \gamma$ (it is the largest statistics for this decay) have been observed in a new kinematical region $25MeV < E^\star_\gamma < 150MeV$. The preliminary result for $F_V - F_A$ is $F_V - F_A = 0.12 \pm 0.03(stat) \pm 0.04(syst)$.

The author would like to thank Vladimir Obraztsov (IHEP, Protvino), Alexey Khudyakov (INR RAS, Moscow) and Andrey Makarov (INR RAS, Moscow) for numerous discussions. The work is supported by Russian Foundation for Basic Research (grant 07-02-00957).

References

[1] J.Bijnens, G.Ecker and J.Gasser, Nucl.Phys. B396, 81 (1993); J.Bijnens et al., "Semileptonic kaon decays", 2nd DAPHNE Physics Handbook, 315 (1994).

[2] C.Q. Geng et al. Nucl.Phys. B684 (2004) 281-317; hep-ph/0306165.

[3] Chuan-Hung Chen et al. Phys.Rev.D77:014004,2008; hep-ph/0710.2971.

[4] S.C.Adler et al. Phys.Rev.Lett.85:2256-2259,2000; hep-ex/0003019.

[5] Y.Akiba et al. Phys.Rev.D32:2911,1985.

[6] A.A.Poblaguev et al. Phys.Rev.Lett.89(2002) 061803.

[7] V.N.Bolotov et al., IHEP preprint 8-98,1998.